

Stress Analysis of Steel Beams Made of Sigma Cross-Section

Maciej Adam Dybizbański^{1*}, Katarzyna Rzeszut¹, Aleksandra Szczepańska¹

¹ Faculty of Civil and Transport Engineering, Poznań University of Technology, ul. Marii Skłodowskiej-Curie 5, 60-965 Poznań, Poland

* Corresponding author's e-mail: maciej.dybizbanski@doctorate.put.poznan.pl

ABSTRACT

This paper presents a stress analysis of elements made of a steel cold-formed sigma cross-section, uniformly loaded in a plane parallel to the web and not passing through the shear centre. Such an application of a load very often occurs in engineering practice and corresponds to the application of a load to the upper flange of the cross-section. It usually results in an additional torsional moment. In this paper, special attention is paid to normal stresses from the bi-moment, and shear stresses from restrained and free torsion. The contribution of these stresses to the section utilization was evaluated on the example of a sigma cross-section with different thicknesses of the wall. Furthermore, the paper also included the stresses analysis concerning different load locations at the upper flange. All numerical calculations were made using analytical approach based on Vlasov beam theory.

Keywords: sigma cross-section, Vlasov theory, warping torsion, bi-moment.

INTRODUCTION

Thin-walled bars, due to the high slenderness of their walls, are sensitive to the loss of stability phenomenon, which is described as a sudden change in shape (deformation) of a structural element under critical load. There are distinguished three basic forms of loss of stability [1, 2], namely global local and distortional. Global beam instability was developed by Vlasov [3] as a well-known Vlasov beam theory, which is based on previous work of Timoshenko [4] and dedicated to the thin-walled steel elements with the open cross-section. The basis to calculate local buckling comes from the theory of plates from [5] and the experimental corrections done by Winter for the preparation of the first edition of the American Iron and Steel Institute Specification for the Design of Cold-Formed Steel Structural Members [6]. For practical reasons, the concepts of the effective width and effective thickness were proposed and introduced in Eurocode [7]. A description of the thin-walled element theory is also described in the works [8, 9]. Despite of

cold-formed steel elements bearing capacity procedures are widely known in engineering practice, there is still a place for further investigations for the cross-sections with one axis of symmetry, such as sigma cross-sections.

As it can be observed, the list of publications referring to sigma cross-sections analysis is very limited. Although, in recent years there has been an increased interest in solutions related to thin-walled, cold-formed steel structures. The latest study by [10] was conducted to describe the behaviour of compressed thin-walled steel columns with a sigma cross-section. The authors of [11] investigated the buckling behaviour of cold-formed steel sigma beam-column members. In their study, the analyses indicate that the failure modes are mainly depending on the stress distribution of the cross-section. The buckling analyses of cold-formed steel sigma cross-sections in purlin-sheeting systems subjected to uniformly distributed uplift load were conducted in [12]. Axially loaded cold-formed sigma profiles were investigated in order to define their local and distortional buckling behaviour [13].

An analytical approach was devised for calculating the bending–torsion coupled random response of thin-walled beams with monosymmetrical cross-sections in [14]. The authors of [15] investigated the Goldenvejzer solution for the system of governing differential equations of stability of centrally loaded members with rigid open cross-sections. Based on a combination of the Vlasov assumption and the Kirchhoff assumption of plate/shell theory, an analytical formulation for the torsional warping function of a thin-walled open-section beam is proposed in [16]. In [17] the authors investigated a simple thin-walled beam carrying a uniformly distributed transverse load. The post-buckling analysis of thin-walled elements with open sections was investigated in [18, 19]. Finite element analysis of thin-walled open section beam structures was presented in [20]. Furthermore, other research in the field of thin-walled elements includes work presented in [21, 22, 23, 24]. However, due to many difficult-to-solve problems, that still have not been discovered despite many years of research, engineers’ usage of thin-walled monosymmetric members is significantly limited. Studies mostly concern topics related to buckling analysis, however, there is a gap in the knowledge of stress analysis of sigma cross-sections. In engineering practice, it is common to neglect the free and restrained torsion components, however, in this paper, the emphasis is placed on analysing the contribution of both free and restrained torsion to the stress block. For these reasons, in this paper, the stress analysis of a sigma cross-section is carried out.

For bending beams of the sigma section, loaded in a plane parallel to the web and not passing through the shear centre, normal stresses from torsional warping σ_ω occur in addition to the normal stresses from bending σ_x . The normal stresses are accompanied by shear stresses from torsional warping τ_ω , uniformly distributed over the wall thickness, which are associated by shear stresses from free torsion τ_i .

In the Vlasov beam theory of restrained torsion, it is assumed that the relationships derived for free torsion are valid. The angle of rotation is defined as:

$$\Theta = \frac{M_T}{GI_T} \tag{1}$$

where: M_T – torsional moment, G – Kirchoff’s modulus, I_T – torsional moment of inertia.

In the case of a profile, which consists of many rectangular parts, the torsional moment of inertia is roughly equal to the sum of torsional moments of individual walls:

$$I_T = a \sum \frac{s\delta^2}{3} \tag{2}$$

where: δ – thickness of a wall, a – width of each wall into which the profile can be separated, s – experimental coefficient, which depends on the shape of a cross-section.

The experimental coefficient is based on results obtained from a laboratory tests by Föppl [25], who computed this parameter for torsion of a narrow rectangular cross-section.

Shear stresses resulting from free torsion, constant in all sections, are defined by formula:

$$\tau_T = \frac{M_T \delta}{I_T} \tag{3}$$

The longitudinal displacement in the coordinate system (x, y, z) of the member section is proportional to the sectional coordinate:

$$u(x, y, z) = -\Theta \omega \tag{4}$$

The axis of rotation during torsion with constrained warping passes through the shear center. During deformation, all the remaining fibers, except those on the axis of rotation, are curved. Since the warping due to varying torsion angles is not constant, elongations $\epsilon_\omega = du/dx$ and normal stresses from warping torsion $\sigma_\omega = E\epsilon_\omega$ arise in the direction of the longitudinal axis of the member. Under the influence of variable normal stresses from warping torsion ϵ_ω , shear stresses from warping torsion τ_ω are evenly distributed over the thickness of the walls.

The lack of freedom of deplaning induces a normal stresses from warping torsion equal to:

$$\sigma_\omega = E \frac{du}{dx} = -E \cdot \frac{d^2 \varphi}{dx^2} \tag{5}$$

where: E – Young’s modulus, φ – section torsion angle.

Additionally:

$$\Theta = \frac{d\varphi}{dx} \tag{6}$$

The normal stresses due to bi-moment are calculated from the formula:

$$\sigma_\omega = \frac{B_\omega \omega}{I_\omega} \tag{7}$$

The shear stresses from warping torsion are calculated according to the following formula:

$$\tau_{\omega} = \frac{M_{\omega} S_{\omega}}{I_{\omega} t} \quad (8)$$

where: B_{ω} – bi-moment, M_{ω} – warping-torsional moment, S_{ω} – sectional static moment, I_{ω} – sectional moment of inertia, t – wall thickness, ω – sectorial coordinate.

The warping-torsional moment is described as:

$$M_{\omega} = \frac{dB_{\omega}}{dx} = -EI_{\omega} \frac{d^3\varphi}{dx^3} \quad (9)$$

Bi-moment is defined as pairs of moments of same amplitude and opposite direction:

$$B_{\omega} = -EI_{\omega} \frac{d^2\varphi}{dx^2} \quad (10)$$

The formula for calculating normal stresses due to normal forces with bending and torsion for a member is:

$$\sigma_x = \sigma_x^N \pm \sigma_x^{M_y} \pm \sigma_x^{M_z} \pm \sigma_x^{B_{\omega}} \quad (11)$$

where: σ_x^N – normal stresses from compression/tension, $\sigma_x^{M_y}$ – normal stresses from bending in respect to “y” axis, $\sigma_x^{M_z}$ – normal stresses from bending in respect to “z” axis, $\sigma_x^{B_{\omega}}$ – normal stresses from torsional warping.

The formula (11) can also be presented as:

$$\sigma_x = \frac{N}{A} \pm \frac{M_y}{I_y} z \pm \frac{M_z}{I_z} y \pm \frac{B_{\omega}}{I_{\omega}} \omega \quad (12)$$

where: N – normal force, A – area of the cross-section, M_y – bending moment in respect to “y” axis, I_y – moment of inertia in respect to “y” axis, z – distance from cross-section’s centre of gravity in respect to “y” axis, M_z – bending moment in respect to “z” axis, I_z – moment of inertia in respect to “z” axis, y – distance from cross-section’s centre of gravity in respect to “z” axis, B_{ω} – bi-moment, I_{ω} – a sectional moment of inertia, ω – sectorial coordinate.

The first three components of the equation (12) correspond to the beam theory regarding compression in combination with bending. The last component contains the bi-moment B_{ω} , the sectional moment of inertia I_{ω} , and the sectorial coordinate ω .

Formula (12) is a generalization of eccentric compression, where the last component defines the normal stresses due to warping. These stresses are distributed in the cross-section according to the concept of the sectoral surfaces.

The formula for calculating shear stresses due to shear forces with bending and torsion for a member with an open profile is:

$$\tau = \tau^{V_z} \pm \tau^{V_y} \pm \tau^{M_{\omega}} \pm \tau^{M_t} \quad (13)$$

where: τ^{V_z} – shear stresses from forces in “z” axis direction, τ^{V_y} – shear stresses from forces in “y” axis direction, $\tau^{M_{\omega}}$ – shear stresses from warping-torsional moment, τ^{M_t} – shear stresses from torsional moment.

The formula (13) can also be presented as:

$$\tau = \frac{V_z S_y}{t I_y} \pm \frac{V_y S_z}{t I_z} \pm \frac{M_{\omega} S_{\omega}}{t I_{\omega}} \pm \frac{M_T t}{I_T} \quad (14)$$

where: V_z – shear force in “z” axis direction, S_y – moment of stability in respect to “y” axis, I_y – moment of inertia in respect to “y” axis, V_y – shear force in “y” axis direction, S_z – moment of stability in respect to “z” axis, I_z – moment of inertia in respect to “z” axis, M_{ω} – warping-torsional moment, S_{ω} – sectional static moment, I_{ω} – a sectional moment of inertia, M_T – torsional moment, I_T – a torsional moment of inertia, t – wall thickness.

PROBLEM FORMULATION

The purpose of the research conducted in this paper was to determine the stress state when considering a load located at the upper flange and not passing through the shear centre. This approach is a departure from the well-known Vlasov beam theory, which assumes that the load is located in a plane passing through the shear centre. The estimation of the contribution of normal and shear stresses from free and restrained torsion to the section was carried out for cold-formed beams made of sigma cross-sections $\Sigma 200 \times 2.00$, $\Sigma 200 \times 2.50$, and $\Sigma 200 \times 3.00$. The calculations were conducted for members with the static scheme of a simply supported beam. The beam span was assumed to be 4 m. A uniform load of 2.00 kN/m along the entire length was considered. The load was applied to the upper flange of the beam in three different plane locations. The first case refers to the situation, where linear load passes through the

middle of the flange width. The second one passes through the quarter of the flange width, and the third passes near the web of the beam. The last one is recommended by EC3 1–3 for gravitational load case, due to high flexural sensibility of the upper flange. Henceforth, an additional torsional moment was considered. The structural elements were made of S350 steel grade. Several geometrical characteristics have been determined following the sigma profile catalogue [26]. Figure 1 presents the geometrical and Figure 2 the load cross-sections schemes of analysed problem.

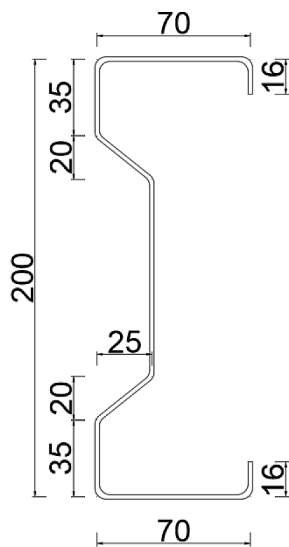


Fig. 1. Geometrical cross-section scheme

STRESS ANALYSIS IN CONTEXT OF VLASOV THEORY

All numerical calculations were carried out for a computational model in accordance with the currently relevant Eurocode, characterised by flat walls with sharp edges. The stress values were calculated for ten points located in the mid span cross-section of the beam, shown in Figure 2.

Consideration of additional torsion

Linear uniformly distributed load was located in the distance as shown in Figure 3. The value of q was assumed as:

$$b_i = (b_1, b_2, b_3) = \left(\frac{b_p}{2}, \frac{b_p}{4}, 0 \right) \quad (15)$$

Linear uniformly distributed load caused the additional torsional moment:

$$m_S = q_p (b_i - y_o + y_{s,sh}) \quad (16)$$

To determine the bi-moment and the torsion angle the following formula was used:

$$\begin{cases} B''_{\omega} - \vartheta \cdot B_{\omega} = m_S \\ \psi^{IV} - \vartheta^2 \cdot \psi'' = \frac{m_S}{E_I I_{\omega}} \end{cases} \quad (17)$$

where:

$$\vartheta^2 = \frac{GI_T}{E_I I_{\omega}} \quad (18)$$

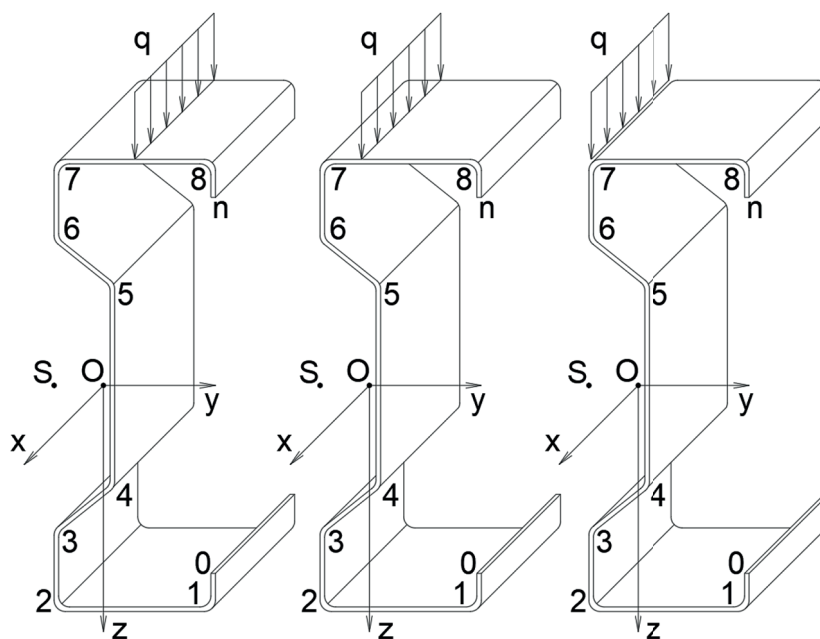


Fig. 2. Loaded sections schemes of the analysed problem

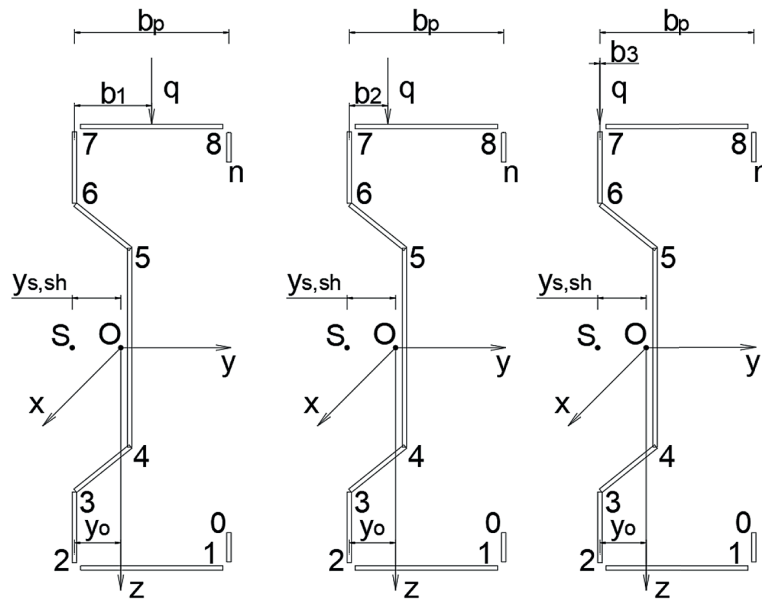


Fig. 3. Location of the calculation points on the beam cross-section

The functions of the bi-moment B_ω and the torsional moment m_s will be calculated after solving the differential equation for the torsion angle ψ . When the factor ϑl is sufficiently small, this equation can be simplified considerably by assuming that $GI_S = 0$. The multiplier GI_S is neglected if:

- for double-sided fork support ($\psi = \psi'' = 0$), $\vartheta l < 0.75$.
- for full restraint on both sides ($\psi = \psi' = 0$), $\vartheta l < 1.50$.
- for one end free and the other fully restrained, $\vartheta l < 0.50$.

The boundary conditions in the considered case for the free-supported beam ($\psi(0) = \psi(1) = 0$, $\psi''(0) = \psi''(1) = 0$) correspond to the fork support conditions. Therefore, the coefficient ϑl was analysed in terms of fork support:

$$\vartheta l = l \sqrt{\frac{GI_T}{E_I I_\omega}} = l \sqrt{\frac{(1 - \nu) I_T}{2 I_\omega}} \quad (19)$$

Due to the support conditions, the differential equation for the torsional angle takes the form:

$$E_I I_\omega \psi^{IV} = m_s \quad (20)$$

The boundary conditions in the considered case ($\psi(0) = \psi(1) = 0$, $\psi''(0) = \psi''(1) = 0$) correspond to those of a simply supported beam ($w(0) = w(1) = 0$, $w''(0) = w''(1) = 0$). Due to this analogy the diagrams of B_ω and M_ω , shown in Figure 4, can be created. With the analogy of a simply supported beam, the formula for the value of the bimoment at mid-span of the beam can be determined:

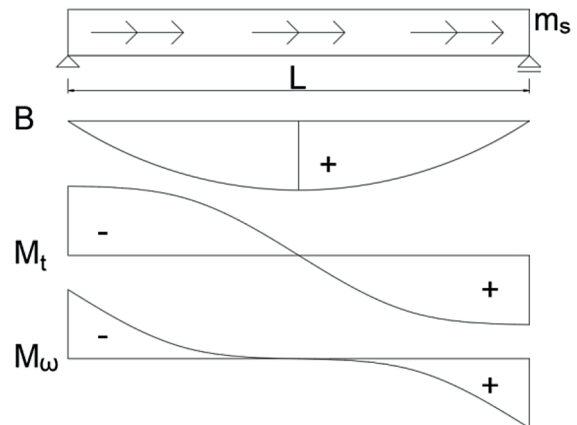


Fig. 4. The diagrams of bi-moment, torsional moment, and torsional warping moment for simply supported beam

$$B_\omega = \frac{m_s l^2}{8} \quad (21)$$

Furthermore, the formula for warping-torsional moment near the beam supports may be specified as:

$$M_\omega = \frac{m_s l}{2} \quad (22)$$

Research program

The process of the analysis was started by the determination of geometrical characteristics of sigma sections considering cross-sections with sharp edges according to [7]. Subsequently, the values of bi-moment, as well as normal and shear stresses, were concluded. Finally, the comparison

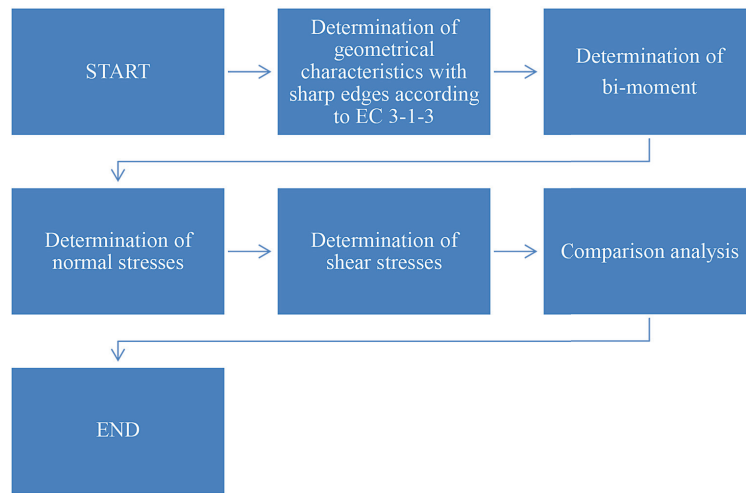


Fig. 5. The flowchart of analysis process

analysis was carried out. Figure 5 shows the flowchart of the analysis process.

Numerical calculations

The results of numerical calculations were collected in Tables 1– 9. Figure 6 presents the diagrams of shear stresses from shear forces and warping torsion, as well as normal stresses from

bending and warping torsion for the one selected case of considered several examples namely $\Sigma 200 \times 2.00$ cross-section for load in the middle of the flange. The shear stresses from shear forces and warping torsion, as well as normal stresses from bending and warping torsion for the one selected case of considered several examples namely $\Sigma 200 \times 2.00$ cross-section for load near the web are presented in Figure 7.

Table 1. Stress values of the $\Sigma 200 \times 2.00$ section – load in the middle of the flange

Section BP/S200x2.00, Span $L = 4.00$ m, Load $q = 2.00$ kN/m, Location $b_1 = b_p/2$				
Point	$\sigma_x^{M_y}$ [MPa]	$\sigma_x^{B_\omega}$ [MPa]	τ_ω [MPa]	τ_{xz} [MPa]
0	80.88	-176.65	0.00	0.00
1	93.64	-144.47	-1.06	1.16
2	93.64	99.33	-1.79	-7.19
3	62.59	101.84	-3.41	-8.23
4	43.33	40.23	-4.55	-9.74
5	-43.33	-40.23	-4.55	-9.74
6	-62.59	-101.84	-3.41	-8.23
7	-93.64	-99.33	-1.79	-7.19
8	-93.64	144.47	-1.06	1.16
N	-80.88	176.65	0.00	0.00

Table 2. Stress values of the $\Sigma 200 \times 2.00$ section – load in the quarter of the flange

Section BP/S200x2.00, Span $L = 4.00$ m, Load $q = 2.00$ kN/m, Location $b_2 = b_p/4$				
Point	$\sigma_x^{M_y}$ [MPa]	$\sigma_x^{B_\omega}$ [MPa]	τ_ω [MPa]	τ_{xz} [MPa]
0	80.88	-82.47	0.00	0.00
1	93.64	-67.45	-0.50	1.16
2	93.64	46.37	-0.84	-7.19
3	62.59	47.54	-1.59	-8.23
4	43.33	18.78	-2.12	-9.74
5	-43.33	-18.78	-2.12	-9.74
6	-62.59	-47.54	-1.59	-8.23
7	-93.64	-46.37	-0.84	-7.19
8	-93.64	67.45	-0.50	1.16
n	-80.88	82.47	0.00	0.00

Table 3. Stress values of the $\Sigma 200 \times 2.00$ section – load near the web (in point 7)

Section BP/S200x2.00, Span $L = 4.00$ m, Load $q = 2.00$ kN/m, Location $b_3 = 0$				
Point	$\sigma_x^{M_y}$ [MPa]	$\sigma_x^{B_\omega}$ [MPa]	τ_ω [MPa]	τ_{xz} [MPa]
0	80.88	11.71	0.00	0.00
1	93.64	9.58	0.07	1.16
2	93.64	-6.58	0.12	-7.19
3	62.59	-6.75	0.23	-8.23
4	43.33	-2.67	0.30	-9.74
5	-43.33	2.67	0.30	-9.74
6	-62.59	6.75	0.23	-8.23
7	-93.64	6.58	0.12	-7.19
8	-93.64	-9.58	0.07	1.16
n	-80.88	-11.71	0.00	0.00

Table 4. Stress values of the $\Sigma 200 \times 2.50$ section – load in the middle of the flange

Section BP/S200x2.50, Span $L = 4.00$ m, Load $q = 2.00$ kN/m, Location $b_1 = b_p/2$				
Point	$\sigma_x^{M_y}$ [MPa]	$\sigma_x^{B_\omega}$ [MPa]	τ_ω [MPa]	τ_{xz} [MPa]
0	65.72	-140.56	0.00	0.00
1	75.84	-115.59	-0.83	0.91
2	75.84	79.11	-1.41	-5.76
3	50.86	81.56	-2.69	-6.57
4	35.21	31.96	-3.60	-7.80
5	-35.21	-31.96	-3.60	-7.80
6	-50.86	-81.56	-2.69	-6.57
7	-75.84	-79.11	-1.41	-5.76
8	-75.84	115.59	-0.83	0.91
n	-65.72	140.56	0.00	0.00

Table 5. Stress values of the $\Sigma 200 \times 2.50$ section – load in the quarter of the flange

Section BP/S200x2.50, Span $L = 4.00$ m, Load $q = 2.00$ kN/m, Location $b_2 = b_p/4$				
Point	$\sigma_x^{M_y}$ [MPa]	$\sigma_x^{B_\omega}$ [MPa]	τ_ω [MPa]	τ_{xz} [MPa]
0	65.72	-64.49	0.00	0.00
1	75.84	-53.03	-0.38	0.91
2	75.84	36.30	-0.65	-5.76
3	50.86	37.42	-1.24	-6.57
4	35.21	14.66	-1.65	-7.80
5	-35.21	-14.66	-1.65	-7.80
6	-50.86	-37.42	-1.24	-6.57
7	-75.84	-36.30	-0.65	-5.76
8	-75.84	53.03	-0.38	0.91
n	-65.72	64.49	0.00	0.00

Table 6. Stress values of the $\Sigma 200 \times 2.50$ section – load near the web (in point 7)

Section BP/S200x2.50, Span $L = 4.00$ m, Load $q = 2.00$ kN/m, Location $b_3 = 0$				
Point	$\sigma_x^{M_y}$ [MPa]	$\sigma_x^{B_\omega}$ [MPa]	τ_ω [MPa]	τ_{xz} [MPa]
0	65.72	11.59	0.00	0.00
1	75.84	9.53	0.07	0.91
2	75.84	-6.52	0.12	-5.76
3	50.86	-6.72	0.22	-6.57
4	35.21	-2.63	0.30	-7.80
5	-35.21	2.63	0.30	-7.80
6	-50.86	6.72	0.22	-6.57
7	-75.84	6.52	0.12	-5.76
8	-75.84	-9.53	0.07	0.91
n	-65.72	-11.59	0.00	0.00

Table 7. Stress values of the $\Sigma 200 \times 3.00$ section – load in the middle of the flange

Section BP/S200x3.00, Span $L = 4.00$ m, Load $q = 2.00$ kN/m, Location $b_1 = b_p/2$				
Point	$\sigma_x^{M_y}$ [MPa]	$\sigma_x^{B_\omega}$ [MPa]	τ_ω [MPa]	τ_{xz} [MPa]
0	55.64	-116.44	0.00	0.00
1	63.98	-96.28	-0.67	0.75
2	63.98	65.60	-1.15	-4.80
3	43.05	68.00	-2.21	-5.47
4	29.81	26.42	-2.97	-6.51
5	-29.81	-26.42	-2.97	-6.51
6	-43.05	-68.00	-2.21	-5.47
7	-63.98	-65.60	-1.15	-4.80
8	-63.98	96.28	-0.67	0.75
n	-55.64	116.44	0.00	0.00

Table 8. Stress values of the $\Sigma 200 \times 3.00$ section – load in the quarter of the flange

Section BP/S200x3.00, Span $L = 4.00$ m, Load $q = 2.00$ kN/m, Location $b_2 = b_p/4$				
Point	$\sigma_x^{M_y}$ [MPa]	$\sigma_x^{B_\omega}$ [MPa]	τ_ω [MPa]	τ_{xz} [MPa]
0	55.64	-52.43	0.00	0.00
1	63.98	-43.36	-0.30	0.75
2	63.98	29.54	-0.52	-4.80
3	43.05	30.62	-1.00	-5.47
4	29.81	11.90	-1.34	-6.51
5	-29.81	-11.90	-1.34	-6.51
6	-43.05	-30.62	-1.00	-5.47
7	-63.98	-29.54	-0.52	-4.80
8	-63.98	43.36	-0.30	0.75
n	-55.64	52.43	0.00	0.00

Table 9. Stress values of the $\Sigma 200 \times 3.00$ section – load near the web (in point 7)

Section BP/S200x3.00, Span $L = 4.00$ m, Load $q = 2.00$ kN/m, Location $b_3 = 0$				
Point	$\sigma_x^{M_y}$ [MPa]	$\sigma_x^{B_\omega}$ [MPa]	τ_ω [MPa]	τ_{xz} [MPa]
0	55.64	11.57	0.00	0.00
1	63.98	9.57	0.07	0.75
2	63.98	-6.52	0.11	-4.80
3	43.05	-6.76	0.22	-5.47
4	29.81	-2.63	0.29	-6.51
5	-29.81	2.63	0.29	-6.51
6	-43.05	6.76	0.22	-5.47
7	-63.98	6.52	0.11	-4.80
8	-63.98	-9.57	0.07	0.75
n	-55.64	-11.57	0.00	0.00

For the same thickness, it can be observed that the normal stresses from warping torsion are roughly 50% higher when the load is positioned in the middle of the flange than when the load is located in the quarter of the flange. However, for the same thickness, the difference is approximately 10–15 times greater when the load is located in the middle of the flange and near the web. Furthermore, the normal stresses from warping torsion for mid-span cross-sections reached approximately 6–10%

of the bending stresses for cases with load near the web. A value of approximately 89–93% was observed for cases with load in the middle of the flange. Finally, for cases with load in the flange quarter, the value ranged between 40 and 43%.

In the case of shear stresses, the stresses force from different load placement was up to about 30 times greater than the shear stresses from warping torsion, depending on the thickness of the wall and load location.

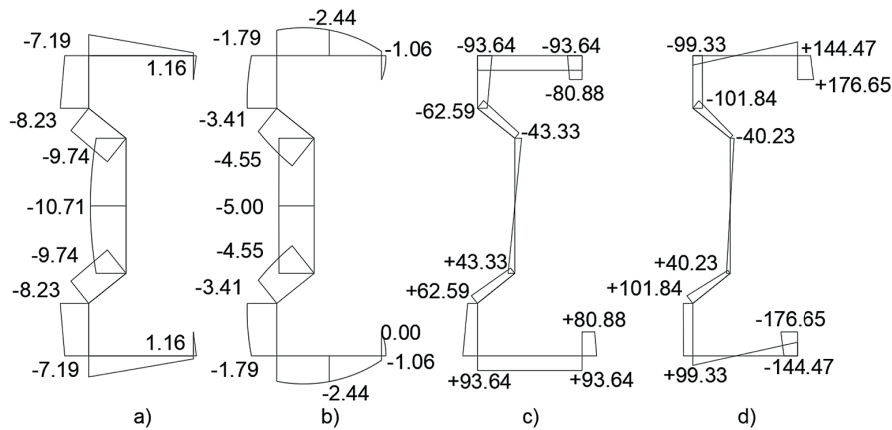


Fig. 6. Diagrams for a) the shear stresses from forces in “z” direction, b) the shear stresses from torsional warping, c) normal stresses from bending, d) normal stresses from torsional warping for $\Sigma 200 \times 2.00$ considering load in the middle of the flange

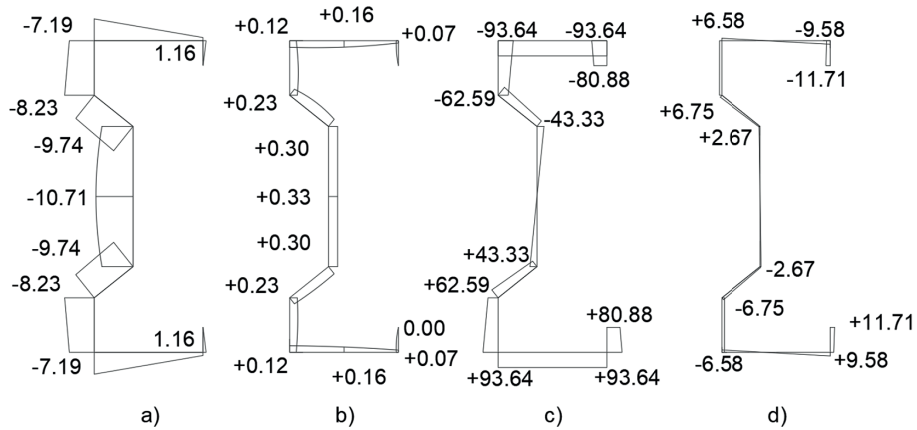


Fig. 7. Diagrams for a) the shear stresses from forces in “z” direction, b) the shear stresses from torsional warping, c) normal stresses from bending, d) normal stresses from torsional warping for $\Sigma 200 \times 2.00$ considering load near the web

By comparing Figures 6 and 7, it is clear that for load close to the web, the normal and shear stress values caused by warping are relatively small and have little importance in bearing capacity, meanwhile for load in the middle of the flange shear and normal stresses from torsional warping are more significant.

FREE AND WARPING TORSION STRESSES

From an engineering and scientific point of view, it seems very interesting to determine the effect of stresses resulting from additional torsion, including warping torsion in the load capacity of the cross-section. Hence the estimation of the contribution of shear stresses determined for warping torsion and shear forces were expressed in the form of the parameter κ :

$$\kappa = \frac{\tau_{\omega}}{\tau_{xz}} \tag{23}$$

Figure 8 shows the parameter change for each point on mid-span sigma cross-sections describing the contribution of shear stresses from warping torsion and shear forces concerning different load locations for $\Sigma 200 \times 2.00$. Similar values may be noted for $\Sigma 200 \times 2.50$ and $\Sigma 200 \times 3.00$.

It should be noted that for the same thickness the load location heavily influences the parameter. Furthermore, the greatest difference in parameter κ can be seen on points 1 and 8, both located on the opposite corner of the cross-section, at the end of the flange.

A similar analysis for load in the middle of the flange was carried out. Figure 9 depicts the variation of the parameter concerning different wall thicknesses of $\Sigma 200$.

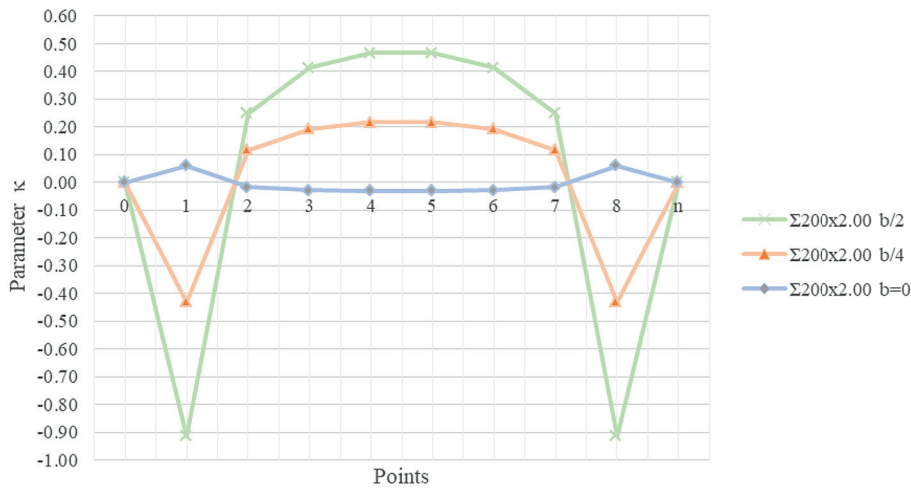


Fig. 8. Contribution of warping torsion and shear forces concerning different load locations for Σ200×2.00

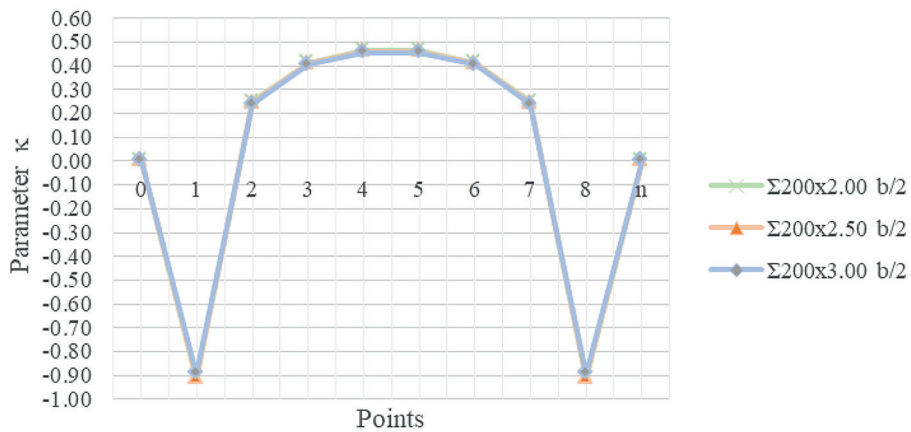


Fig. 9. Contribution of warping torsion and shear forces to load in the middle of the flange for different wall thicknesses of Σ200

For the load located at the centre of the flange, the parameter κ is not much different, which proves that in this case, the section thickness has little effect on the shear stresses from warping torsion and shear forces. Figure 10 depicts the κ parameter values for each point on mid-span sigma cross-sections, demonstrating how different wall thickness of S200 affects warping torsion and shear forces for load located near the web.

The parameter κ for the load near the end of the flange varies considerably with wall thickness. The greatest differences in contribution between shear stress from warping torsion and shear force from load location can be observed for the thickest wall.

Overall, it can be concluded that the influence of shear stresses from warping torsion τ_ω is theoretically not so significant, however it should not be neglected in the case of the sigma

cross-section, as it differs with different load location. Moreover, it is especially critical for elements with thicker walls and the load located close to the web.

In next step, in order to formulate the relation between the normal stresses caused by warping and bending the parameter was formulated:

$$\rho = \frac{\sigma_\omega}{\sigma_x} \tag{24}$$

A normal stresses ratio is represented in Figure 11 for points located on mid-span sigma cross-section for Σ200×2.00 with respect to the different load location.

For the load located in the middle of the flange, the normal stresses from warping torsion were up to approximately 220% of the stresses from bending, as it can be observed in Figure 11. Furthermore, it was found that for load location near the web, the normal stresses

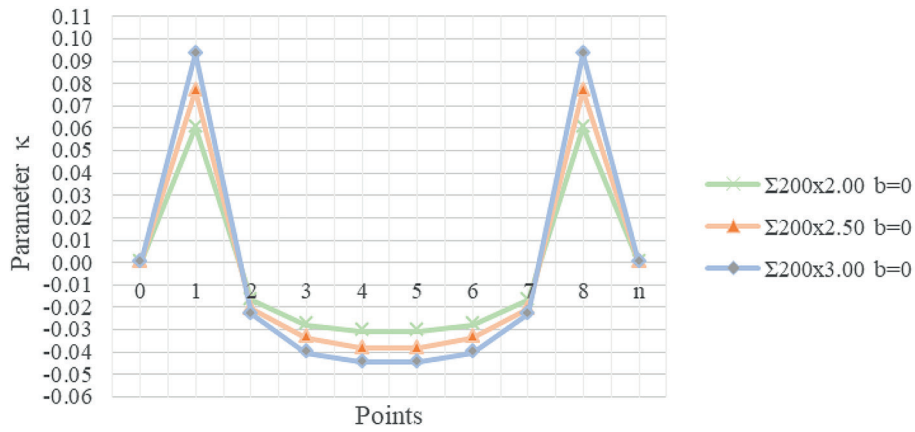


Fig. 10. Contribution of warping torsion and shear forces to load near the web for different wall thicknesses of $\Sigma 200$ (in point 7)

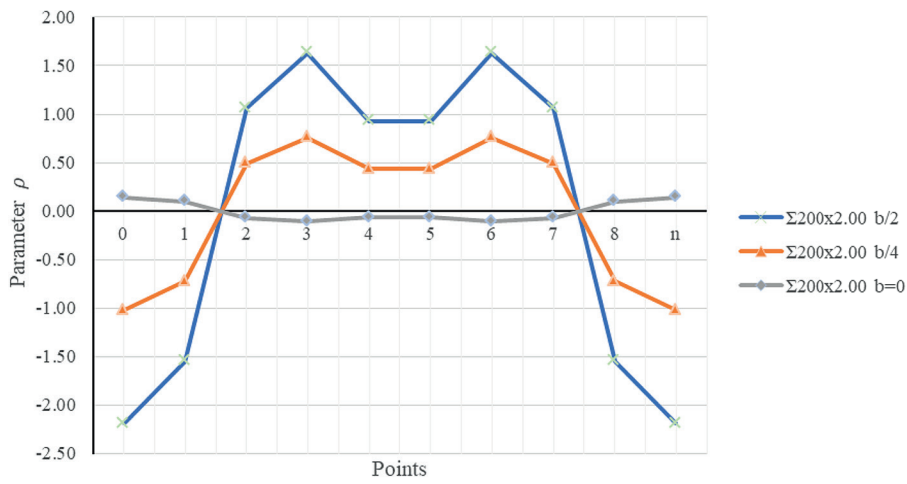


Fig. 11. Comparison of normal stresses caused by warping torsion and bending concerning different load locations for $\Sigma 200 \times 2.00$

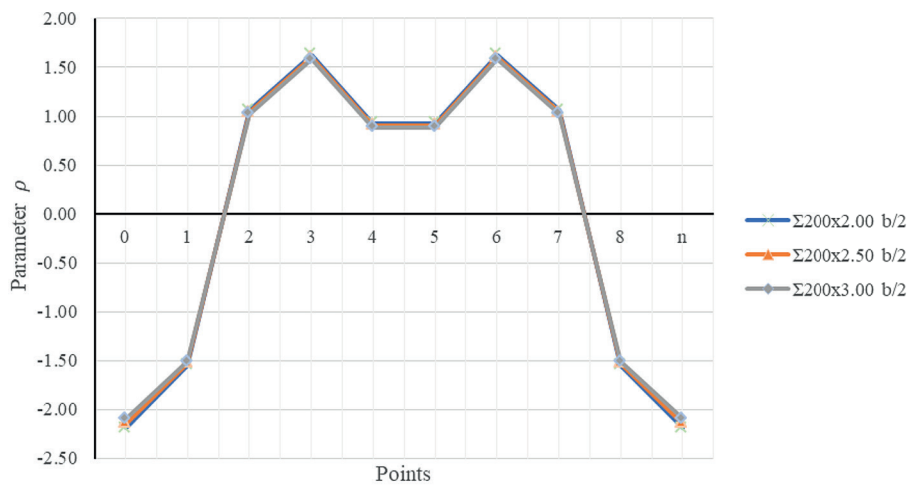


Fig. 12. Comparison of warping torsion and free normal stresses concerning different wall thickness of $\Sigma 200$ for load in the middle of the flange

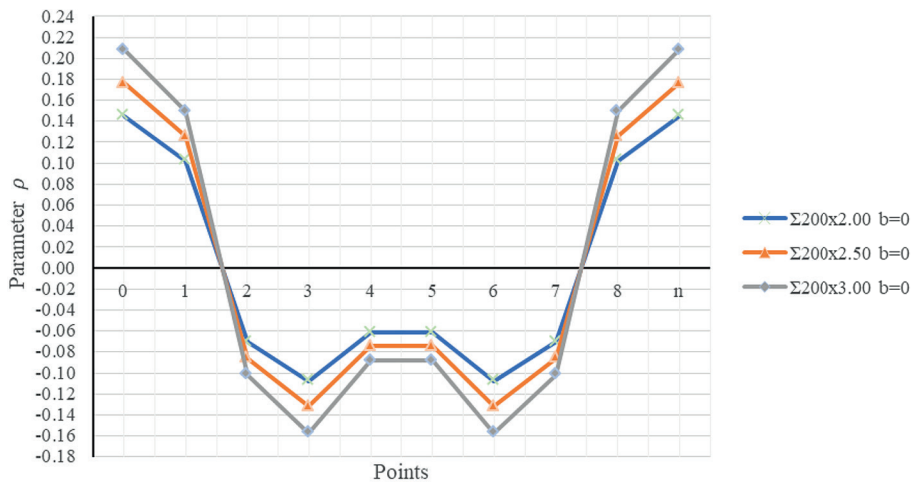


Fig. 13. Comparison of warping torsion and free normal concerning different wall thickness of Σ200 for load near the web (in point 7)

from warping torsion are close to 0 and may even change their direction.

As it is seen in Figure 12, the normal stresses from warping torsion were up to about 220% of stress from bending for the load located in the middle of the flange. Additionally, no significant difference between for each thickness can be noted.

For the load location near the web, the normal stresses from warping torsion were up to about 21% of stresses from bending, as shown in Figure 13. Moreover, the results of this analysis reveal that in comparison the impact of normal stresses from warping torsion σ_w is greater than the impact of shear stresses caused by warping torsion τ_w , especially in the case when load is placed near the web.

CONCLUSIONS

The article presents an analysis of the stress state referring to the theory of thin-walled members, considering the normal and shear stresses from bending and torsion for three different sigma sections: Σ200×2.00, Σ200×2.50, and 200×3.00. Furthermore, a stress analysis of the different load locations at the upper flange was performed. Such a load application, as typical engineering practice, caused the additional torsional moment which should not be neglected. As an outcome, special attention was focused, in the paper, on bearing capacity of normal and shear stresses from warping torsion. It is worthy to note, that this analysis provides important insight into the complex relationship between normal stresses and shear stresses induced by warping. Moreover, it can be used to

develop an accurate bearing capacity approach for the sigma cross-section.

Based on the conducted examples, it was determined that the change in the location of the external load at the upper flange results in the reasonably large increase in stresses caused by warping. Based on the coefficient, developed in order to define the contribution of the shear stresses caused by warping torsion and shear forces, it was found that the warping shear stresses increased for the load location in the middle of the flange. Simultaneously, based on the coefficient, introduced respectively to define the contribution of the normal stresses caused by warping and bending, one can noticed, the similar phenomenon.

Additionally, in the paper, the influence of the wall thickness on the distribution of stresses was investigated. It can be noted, that for the thicker wall the increase in warping, as well for the normal and shear stresses, is observed.

Therefore, it should be pointed out, that the effect of warping definitely has to be taken into account in the case of the sigma cross-section. Thus neglecting the shear and normal stresses caused by warping can lead to the reasonably large mistakes. Moreover, the thickness of the wall can play significant influence, especially when the load is located close to the web.

Acknowledgements

This paper was financially supported by Poznan University of Technology: 0412/SBAD/0060, 0412/SBAD/0061.

REFERENCES

1. Rzeszut K. Stability of thin walled metal structures with clearances and initial imperfections. Wydawnictwo Politechniki Poznańskiej, Poznań, 2015.
2. Bródka J., Broniewicz M., Giżejowski M. Cold formed profiles. Rzeszów: Polskie Wydawnictwo Techniczne; 2006.
3. Vlasov V. Thin-walled elastic beams. Israel Program for Scientific Translations, Jerusalem, 1963.
4. Timoshenko S., Gere J. Theory of elastic stability. McGraw-Hill, New York, 1961.
5. Karman T.V., Sechler E.E., Donnell L.H. The strength of thin plates in compression. Trans. A.S.M.E. 1932; 54: 53–57.
6. American Iron and Steel Institute. Specification for the Design of Light Gage Steel Structural Members; 1946.
7. EN 1993-1-3: Eurocode 3 - Design of steel structures - Part 1–3: General rules – Supplementary rules for cold-formed members and sheeting.
8. Piechnik S. Thin-walled members. Politechnika Krakowska, Kraków, 1992.
9. Rutecki J. Strength of thin walled structures. PWN, Warszawa, 1957.
10. Zhang P., Alam M. Compression tests of thin-walled cold-formed steel columns with Σ -shaped sections and patterned perforations distributed along the length. Thin-Walled Structures. 2022; 174: 109082.
11. Öztürk F., Mojtabaei S., Şentürk M., Pul S., Hajirasouliha I. Buckling behaviour of cold-formed steel sigma and lipped channel beam–column members. Thin-Walled Structures. 2022; 173: 108963.
12. Ren C., Liu X., He W., Dai L. Buckling analyses of cold-formed steel Sigma sections in purlin-sheeting systems subjected to uniformly distributed uplift loading. Structures. 2021; 34: 2262–2275.
13. Ciesielczyk K., Rzeszut K. Local and Distortional Buckling of Axially Loaded Cold Rolled Sigma Profiles. Acta Mechanica et Automatica. 2016; 10(3): 218–222.
14. Jun L., Rongying S., Hongxing H., Xianding J. Response of monosymmetric thin-walled Timoshenko beams to random excitations. International Journal of Solids and Structures. 2004; 41(22–23): 6023–6040.
15. Kovac M., Balaz I. Stability of centrally loaded members with monosymmetric cross-section at various boundary conditions. Journal of Constructional Steel Research. 2019; 153: 139–152.
16. Lin W., Hsiao K. More general expression for the torsional warping of a thin-walled open-section beam. International Journal of Mechanical Sciences. 2003; 45(5): 831–849.
17. Magnucki K., Szyc W., Stasiewicz P. Stress state and elastic buckling of a thin-walled beam with monosymmetrical open cross-section. Thin-Walled Structures. 2004; 42(1): 25–38.
18. Mohri F., Azrar L., Potier-Ferry M. Flexural–torsional post-buckling analysis of thin-walled elements with open sections. Thin-Walled Structures. 2001; 39(11): 907–938.
19. Mohri F., Azrar L., Potier-Ferry, M. Lateral post-buckling analysis of thin-walled open section beams. Thin-Walled Structures. 2002; 40(12): 1013–1036.
20. Dvorkin E., Celentano D., Cuitiño A., Gioia, G. A Vlasov beam element. Computers & Structures. 1989; 33(1): 187–196.
21. Pezeshky P., Sahraei A., Rong F., Sasibut S., Mohareb M. Generalization of the Vlasov theory for lateral torsional buckling analysis of built-up monosymmetric assemblies. Engineering Structures. 2020; 221: 111055.
22. Rajkannu J., Jayachandran S. Flexural-torsional buckling strength of thin-walled channel sections with warping restraint. Journal of Constructional Steel Research. 2020; 169: 106041.
23. Szychowski A. A theoretical analysis of the local buckling in thin-walled bars with open cross-section subjected to warping torsion. Thin-Walled Structures. 2014; 76: 42–55.
24. Sapountzakis E. Bars under Torsional Loading: A Generalized Beam Theory Approach. ISRN Civil Engineering. 2013; 2013: 1–39.
25. Föppl A. Vorlesungen über technische Mechanik: Festigkeitslehre. 1897; 3.
26. Profile Sigma - Profile Z, C, Σ - Pruszyński [Internet]. Profile Sigma - Profile Z, C, Σ - Pruszyński. 2022 [cited 7 November 2021]. Available from: <https://pruszynski.com.pl/profile-sigma,prod,81,51.php>